# A Brillouin scattering study of the glass transition in sucrose

T.J.C.Hosea, S.C.Ng and C.G.Oates[1]

*Department of Physics, National University of Singapore, Singapore 0511 and [1]Department of Biochemistry, National University of Singapore, Singapore 0511, Republic of Singapore*

**Abstract.** The Brillouin laser light scattering spectra of aqueous sucrose solutions have been measured as a function of temperature through the glass transition region. The Brillouin shift and width, which are proportional to the velocity and attenuation of sound waves in the system, respectively, both exhibit marked changes in their temperature coefficients near the glass transition temperature of a sucrose solution containing 30% w/w water. Phase separation behaviour has also been observed in the sucrose solutions.

## Introduction

When amorphous systems are warmed they may undergo a transition from a brittle vitreous state to a viscous liquid or elastic rubbery state. The temperature near which this transition takes place is termed the glass transition temperature $T_g$. The importance of such transitions in food systems is without dispute. Quite apart from the obvious differences in texture between glassy and viscoelastic states, whether or not a food substance is in a glassy state can also influence its 'spoilage' properties; processed foods spoil due to chemical (i.e. browning oxidation), enzymatic, microbial and physical (i.e. recrystallization) processes. Knowledge of $T_g$ is particularly important in freeze drying and freezer storage (1). At temperatures below $T_g$ the food substance may exist as a 'dynamically constrained' amorphous solid (2) which can act as a barrier to ice crystal formation.

Several techniques are commonly used to detect the changes which occur at the glass transition and to measure $T_g$, including differential scanning calorimetry (DSC), differential thermal analysis (DTA), thermal mechanical analysis (TMA) and rheological measurements. DSC is the technique probably most commonly used to identify glass transitions. Here a glass transition is frequently identified from a step change in the thermogram and $T_g$ is determined from the mid-point of the step change as measured from the baselines extrapolated from below and above the transition region. However, the presence of such DSC baseline shifts as sufficient evidence for the existence of a glass transition is an interpretation not without its controversy (3). In some cases it is desirable to have corroborative evidence that the observed thermal events are indeed due to glass transitions.

We have used the technique of Brillouin light-scattering spectroscopy to study transitions in various polymeric substances, including sol–gel systems (4) and glassy materials (5), with some measure of success. However, to our knowledge, the technique has never been applied to study glass transitions in food systems.

137

In order to explore the potential of Brillouin spectroscopy to characterize glass transitions in such materials we undertook a study of several common basic food substances including starches and various oligosaccharides, in which inter- and intra-molecular hydrogen bonds restrict molecular mobility. An increase in the numbers of these bonds causes an increase in $T_g$ (6). Monosaccharides and oligosaccharides exhibit a range of hydrogen bonding potentials, as they exist in a range of conformations. It is of interest, therefore, to obtain accurate measurement of $T_g$ in these materials. To be good candidates for a Brillouin study of their glass transitions, food materials must satisfy several criteria, not the least of which is the requirement that the materials be reasonably optically homogeneous and translucent both above and below $T_g$. Since certain aqueous solutions of sucrose satisfy this requirement and also display strong DSC events (S.Ablett, personal communication) they represent exemplary systems for an initial study.

## Materials and methods

Sucrose–water solutions at various concentrations were prepared by dissolving dry Analar grade sucrose (BDM Chemicals, Ltd) in distilled deionized water at 95°C. The samples were then checked for their suitability for the Brillouin study by visually observing their clarity, first near room temperature and then at low temperatures by rapid quenching in liquid nitrogen. It was found that optically clear samples could not be prepared by the above method if the moisture content was <~20% w/w, due to the difficulty in dissolving the sucrose and subsequent precipitation/crystallization on cooling back to room temperature. Samples with a higher water content were optically very clear but, upon rapid quenching, invariably cracked into many small fragments (which in itself is an indication of a glassy state). However, the fragments themselves would generally remain transparent provided the original liquid was initially clear at room temperature. More careful experiments with somewhat less vigorous quenching revealed that the cracking could be made less severe and that clear optical paths through the frozen specimens could be found. Evidently, the water component of the solutions remained unfrozen in the glassy state (2). When the quenched samples were slowly warmed towards room temperature they would become increasingly cloudy near $T_g$. This turbidity worsened as temperature was further increased and, for specimens with high water content, became prohibitive, eventually making the samples completely opaque and therefore rendering them virtually useless for our Brillouin experiments. Although all the sucrose–water concentrations studied displayed this cloudiness, it was less severe for samples with water contents below about 40% w/w. Hence, it was determined that the most suitable sucrose–water solutions for the Brillouin study lay in the relatively narrow concentration range of roughly 20–40% w/w of water. For the present initial Brillouin study, and to serve as an inceptive demonstration of the technique, a sample containing 30% w/w of water was chosen. This concentration has a $T_g$ of 209 K as measured recently by DSC techniques (S.Ablett, personal communication).

The specimen was poured into a glass tube (i.d. 5 mm) which was sealed with a small air space above the liquid. The tube was inserted inside a closely fitting copper block which had four small apertures to permit light scattering experiments. The copper block was mounted in a combined optical cryostat/ furnace system. The specimen temperature, controlled to within 0.1°C by an Oxford Instruments ITC4 temperature controller, was measured with a copper–constantan thermocouple and a platinum resistance sensor both attached to the copper block close to the glass tube. The sample temperature was changed in steps and held constant for an equilibration time of ~30 min during which the Brillouin spectrum was measured.

The sample was illuminated by a Spectra Physics argon-ion laser operated in single mode (linewidth ≈100 mHz) at a wavelength of $\lambda = 514.5$ nm and a power of typically 80 mW. The light scattered through an angle of $\theta = 90°$ was analysed using a Burleigh DAS-1 five-pass Fabry–Perot interferometer operated with an optimized free spectral range of 37.04 GHz and finesse of 42, as described in detail elsewhere (4). (The optical rotation exhibited by sucrose solutions was unimportant for our measurements of unpolarised Brillouin scattering.) The resulting digital Brillouin spectra were transferred to a microcomputer for processing and analysing.

Brillouin spectroscopy essentially measures the speed and attenuation of hypersonic acoustic waves in the system under study. A small fraction of the incident laser light is shifted both up and down in frequency from its original value due to interactions between the incident light and the local density variations caused by the propagating sound waves. The interferometer accurately measures the intensity of this scattered light as a function of frequency. The resulting Brillouin spectrum consists of a strong narrow central peak, representing unshifted elastic scattering at the incident laser frequency (the Rayleigh scattering), and two much weaker and broader Brillouin sideband peaks displaced symmetrically about the Rayleigh peak, representing the portion of incident light scattered and frequency-shifted by the acoustic sound waves in the system. The amount of this frequency shift (the Brillouin shift $\nu_B$) depends on the speed of sound $v$, the refractive index $n$ and the scattering angle $\theta$ of the system, as given by the relation

$$\nu_B = \frac{2nv}{\lambda} \sin{(\theta/2)} \qquad (1)$$

If the sound waves are spatially damped according to exp $\{-\gamma x\}$, where $\gamma$ is the sound absorption coefficient, then, provided the damping is not too large, the Brillouin sidebands have peak frequencies very near $\pm\nu_B$ and have a FWHM $\Gamma_B$ (full width at half maximum) given by

$$\Gamma_B = \gamma v/\pi \qquad (2)$$

However, any measured Brillouin spectrum is the result of an unavoidable convolution between the true line shape and the instrumental response. The

primary effect of this is to increase appreciably the apparent FWHM of the Brillouin peaks. In the present study the effects of instrumental resolution were removed using an iterative convolution and least-squares fitting procedure assuming a Lorentzian lineshape for the true spectrum (7):

$$I(\nu) = \frac{I_0}{1 + [2\,(\nu - \nu_B)/\Gamma_B]^2} \tag{3}$$

where $\nu$ is the frequency shift and $I_0$ the intensity of the Lorentzian at its peak, where $\nu = \nu_B$.

**Results and discussion**

The Brillouin spectra were measured in two slow temperature stepping sequences.

Firstly, after quenching the sample rapidly from room temperature to ~129 K (at a rate of ~6 K/min), the Brillouin spectra were measured at various fixed temperatures, which was raised in steps through $T_g$ to a final value of 295 K, this heating process taking overall ~7 h. As temperature was raised past 200 K, the intensity of the Brillouin spectra dwindled steadily, as expected, due to the progressively increasing cloudiness of the sample near $T_g$. Here, the samples appeared under laser illumination to be suffused with a uniform milky iridescence, or opalescence. Above ~217 K it proved very difficult to detect the Brillouin signal until the sample cleared suddenly at 258 K, at which point measurement of the spectra was resumed.

In view of these difficulties, the Brillouin spectra were also measured in the reverse of the above sequence, i.e. as a function of temperature lowered in steps from room temperature to about 118 K. It might seem at first sight that such a slow cooling rate (averaging out to ~0.5 K/min in this case) cannot properly be considered as 'quenching' and that there is an increased likelihood of crystals forming in the slowly cooling liquid. One might expect, therefore, that the best one could hope for would be a crystalline/vitreous mixture for the frozen sample. However, even at room temperature, the present pure aqueous solutions of sucrose crystallize extremely slowly (taking typically days for the first small crystals to form). This rate of crystallization is too sluggish to reduce appreciably the degree of disorder and vitreosity in the final state of the frozen material, even for the slow cooling rates necessary for the second Brillouin experiment. Furthermore, in contrast to the heating sequence, the sample did not become turbid during slow cooling but retained its original clarity to well below $T_g$, enabling the Brillouin spectra to be measured reliably over the complete range of temperature.

It should perhaps be remarked that, in both the heating and cooling sequences, the sample cracked in the vitreous state. However, it proved possible to find clear optical paths through the specimen.

Figure 1 depicts the method by which a typical Rayleigh–Brillouin spectrum was computer analysed. It should be noted that only one of the Brillouin
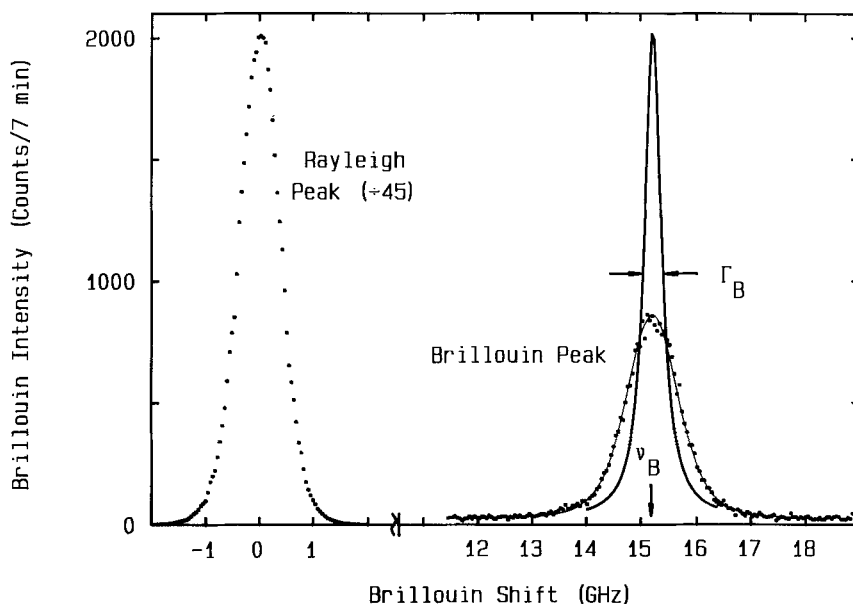
**Fig. 1.** A typical digital Rayleigh–Brillouin spectrum of the aqueous sucrose solution, containing 30% w/w water, at a temperature of 211.1 K. The intense Rayleigh peak has been scaled down by a factor of 45. The figure is more fully explained in the text. Note the break in scale on the horizontal frequency axis.

sidebands is displayed. The measured Brillouin peak, shown as full circles on the right-hand side of the figure, was least-squares fitted with a profile given by convolving a Lorentzian line shape, representing the true spectrum, with the measured instrumental resolution function, which was obtained from the Rayleigh peak, shown on the left-hand side of the figure. A sloping linear background is included in the fit to describe any weak underlying non-resonance scattering. The parameters of the Lorentzian and the background are optimized to obtain the 'best' fit to the experimental data. The fitted profile is shown in the figure as a fine line passing through the experimental points and the resulting deconvolved true spectrum (the Lorentzian) as the bold line. The fitted true Brillouin shift $\nu_B$ is equal to the resonance peak frequency of this optimized Lorentzian profile, and the fitted true Brillouin width $\Gamma_B$ is equal to its full width at half the maximum intensity. Both these quantities are indicated on Figure 1. Note that, while the measured and true spectra have essentially the same peak frequency, their FWHMs differ markedly due to the broadening effect of the instrument.

Figure 2 shows some typical experimental Brillouin spectra for various temperatures, both above and below $T_g$. The Rayleigh peak is not displayed in this figure. It is evident from these spectra that both the Brillouin shift and FWHM undergo marked changes between the glassy and viscoelastic states.

Figure 3 shows the results obtained for $\nu_B$ from the computer analysis of the spectra obtained in both the heating and cooling sequences. It is clear that $\nu_B$
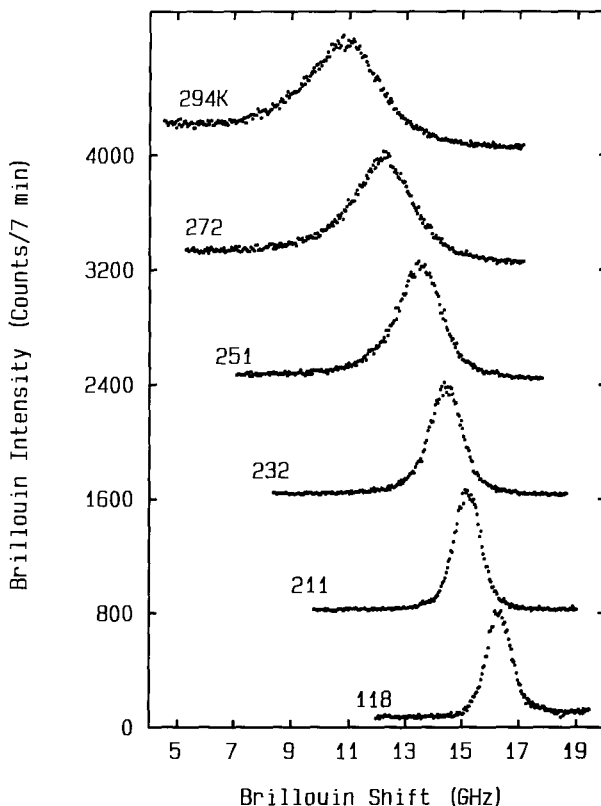
141

**Fig. 2.** Some typical digital Brillouin spectra of the aqueous sucrose solution, containing 30% w/w water, for various temperatures above and below the glass transition. The temperatures (in K) are indicated next to each spectrum. For the purposes of clarity each spectrum is shifted vertically from its predecessor by 800 counts.

behaves in a nearly linear fashion with temperature well above and well below $T_g$, with a marked change in slope between these two regions. A slope change near $T_g$ in $\nu_B$ [and therefore in the sound velocity $\nu$—see equation (1)] is by now a well-known effect and has been used to identify $T_g$ by workers who have examined polymers by Brillouin scattering (8). It is due to a discontinuity in the temperature coefficient of the specific volume (thermal expansion coefficient) upon which $\nu$ depends (8). Below $T_g$ molecules have almost completely lost translational and rotational motion but retain vibrational motion. Hence, the coefficient of expansion in the vitreous state is lower in comparison to that of the viscoelastic state, above $T_g$, where the molecules have regained their rotational and translational degrees of freedom. The lines in Figure 3 show linear regressive fits to the two regions for the cooling sequence data. Their intersection, which occurs at a temperature of 215 ± 2 K, gives an indication of the glass transition temperature $T_g$, shown in Figure 3 by the arrow. The ratio of the slopes above and below $T_g$ is 6.7.
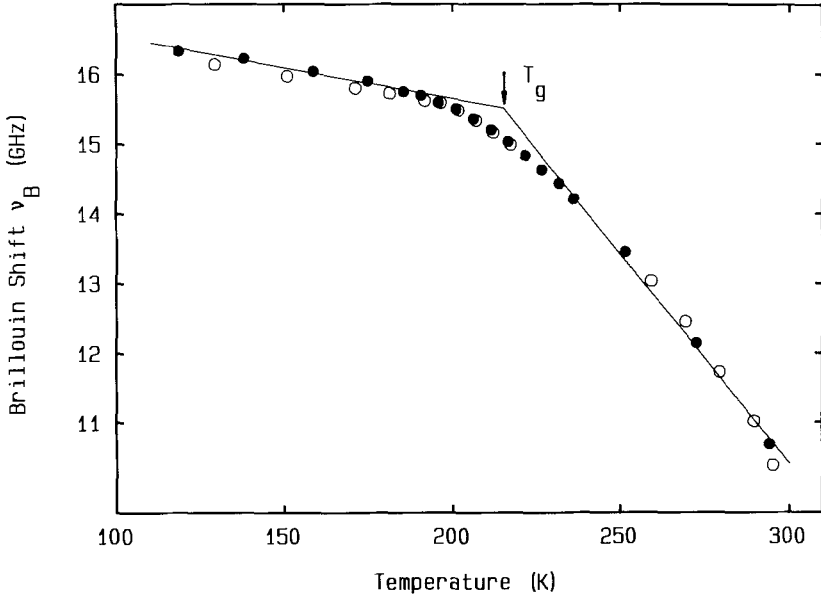
**Fig. 3.** The temperature dependence of the Brillouin shift obtained from the least-squares computer analysis of the Brillouin spectra for the aqueous solution of sucrose for the heating ($\bigcirc$) and cooling ($\bullet$) sequences. The experimental uncertainty in $\nu_B$ is indicated by the size of the symbols. The lines are explained in the text.
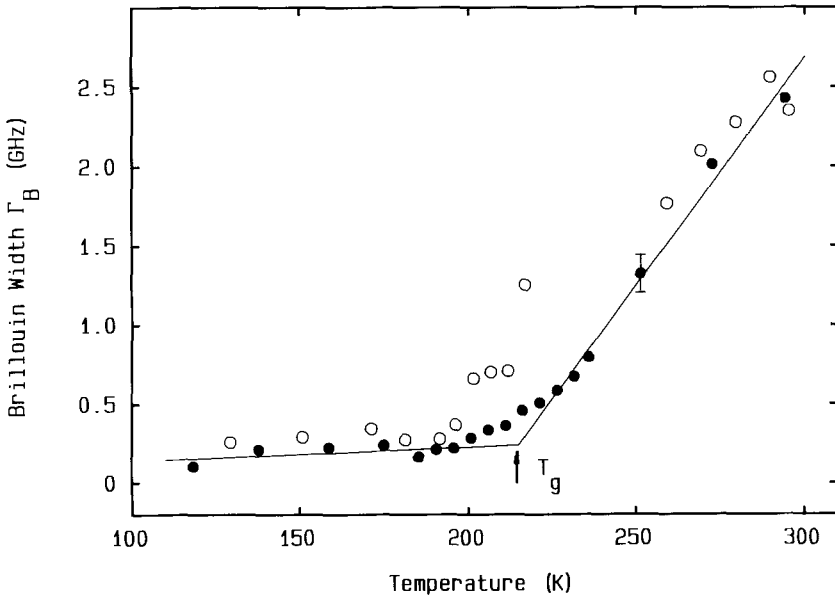


**Fig. 4.** The temperature dependence of the Brillouin width obtained from the least-squares computer analysis of the Brillouin spectra for the aqueous solution of sucrose for the heating ($\bigcirc$) and cooling ($\bullet$) sequences. The bar indicates a typical experimental uncertainty in $\Gamma_B$. The lines are explained in the text.

Figure 4 shows the results for the true Brillouin FWHM $\Gamma_B$. Similar to the situation described above for $\nu_B$, the behaviour of $\Gamma_B$ with temperature is also nearly linear well above and well below $T_g$, with a marked slope change near $T_g$. The lines show linear regressive fits to these two regions for the cooling sequence, with an intersection at a temperature of $215 \pm 1.4$ K, the same as was obtained for $\nu_B$. However, the change in slope is of the opposite sign to that for $\nu_B$ and is much greater in magnitude, the ratio between the slopes above and below $T_g$ being 11.0.

The fact that the slope changes in $\Gamma_B$ and $\nu_B$ $(\nu)$ are in the opposite direction implies that the temperature dependence of the sound absorption coefficient $\gamma$ is not only similar to, but is also stronger than, that of $\Gamma_B$ [see equations (1) and (2)]. The slope change in $\Gamma_B$ $(\gamma)$ may be interpreted as follows. The glass transition region can be considered as the onset of long-range co-ordinated translational and rotational motion of the molecules. Below $T_g$ the sucrose molecules are 'frozen' in random conformations and are virtually immobile (9), apart from vibrational motion around their arrested positions (10). Above $T_g$, the increased thermal energy enhances particle mobility, excites molecular rotational motion and also permits more and more molecules to translate and slide by one another as the system becomes viscoelastic (11). The slope discontinuity in $\Gamma_B$ $(\gamma)$ near $T_g$ may be attributed to the increase in sound scattering due to this long-range co-ordinated molecular motion above $T_g$. Similar effects have been observed by us in the Brillouin spectra of other systems undergoing glass transitions (5).

It is evident from Figures 3 and 4 that, apart from the region between 217 and 258 K, which is missing from the heating sequence, the heating and cooling sequences give the same results within experimental accuracy for $\nu_B$ at all temperatures and for $\Gamma_B$ for the temperature regions in which the sample is transparent. This fact indicates that, as far as the Brillouin spectra are concerned, the nature of the glassy states obtained through rapid quenching and slow cooling are essentially identical. This gives support to our contention that the slow cooling sequence yielded the same glassy state as obtained through rapid quenching.

It may be noted from Figure 4, however, that there is an obvious difference between the two sets of values for $\Gamma_B$ in the temperature range between ~200 K and 220 K. Here, the Brillouin peaks measured during the heating sequence, where the sample is turbid, become increasingly broader in comparison to their counterparts in the cooling sequence. Although part of this effect might be due to the lowered signal-to-noise ratios for the turbid samples, the milky iridescence and increased broadening are both consistent with the interpretation that the sample is undergoing a phase separation behaviour when warming through this temperature region. Liquid systems undergoing such phase transformations/ separations can display such a milky iridescence, due to the reflection of light from the very fine suspension of one phase in the other. Sound waves propagating through this system experience greater scattering due to the increased inhomogeneity of the sample. As a result the Brillouin peak is broadened. Only when the temperature is raised further does the viscoelastic

binary mixture coalesce, to be replaced by the original aqueous sucrose solution. However, Brillouin scattering is not well-suited for a detailed study of phase separation phenomena.

The fact that turbidity is observed between ~210 and 260 K in the heating sequence following the rapid quench, but not in the cooling sequence, is a very interesting phenomenon. One would actually expect that a simple phase separation would not depend on thermal history. On the other hand, if the system displayed metastable behaviour, one might expect phase separation to be more likely to occur during slow cooling than in the heating sequence. A plausible explanation of the observed behaviour, based on the assumption that the phase separation mechanism is due to spinodal decomposition, is given below. When the sample has been quenched to well below the spinodal temperature of the system, it is unstable against small fluctuations in composition and phase separation might be expected to occur. However, diffusion is required for this to happen. The rate of this diffusion, already slow because of high solute content, becomes even slower as temperature is lowered. During the heating sequence, starting from the quenched temperature, phase separation does not take place within a practical timeframe until the temperature is raised sufficiently high to facilitate the required diffusion process. Evidently it actually occurs in the system studied near the spinodal temperature of ~210 K. The sample clears again when its temperature is raised above the binodal temperature of about 260 K. By contrast, during the slow cooling sequence, when the temperature is lowered to between the binodal and spinodal temperatures, the sample enters a metastable region where the mechanism responsible for phase separation is nucleation and growth. However, in order that the system can separate into two phases it is necessary that a nucleus of the proper composition be created. Such nuclei may occur only very rarely or perhaps not at all and the sample will not then phase separate in this region. When the temperature is further lowered to below the spinodal temperature, the rate of cooling, though slow, is still rapid enough to prevent phase separation by spinodal decomposition. Here, every step of cooling further slows down the rate of diffusion which in turn decreases the chances of phase separation. This is quite contrary to the heating sequence where each step of warming speeds up the rate of diffusion leading to an enhancement of the likelihood of phase separation. This is, we believe, why phase separation is observed in the heating sequence but not in the cooling sequence.

## Conclusions

The behaviour of the Brillouin shift $\nu_B$ and width $\Gamma_B$ as a function of temperature in the present concentration of the aqueous sucrose solution has confirmed that the system undergoes a glass transition near $215 \pm 2$ K. This temperature is reasonably close to the value of 209 K as determined by recent DSC measurements (S.Ablett, personal communication). The difference might be either simply attributable to experimental uncertainties (which for the recent DSC results are not known to us) or to the different ways of interpreting the

experimental measurements for the purposes of identifying $T_g$. Experimental determinations of $T_g$ for D-glucose have produced a range of results (280–305 K). It has been suggested that such differences might also arise as a result of different time-scales of the measurements (12).

Determination of $T_g$ by $\nu_B$ alone offers no advantage over conventional techniques. However, since the slope change near $T_g$ in $\Gamma_B$ is more pronounced, the resulting $T_g$ is more reliable. The fact that both values of $T_g$ are, in the present case, the same—215 K ± 2 K—suggests that Brillouin spectroscopy can provide an objective determination of $T_g$ in glassy food systems. The slope changes observed in $\nu_B$ and $\Gamma_B$ can be unambiguously associated with glass transition behaviour. Hence, Brillouin spectroscopy can also provide corroborative evidence that the occurrence of other phenomena, such as thermal baseline shifts observed in DSC experiments, are indeed correctly interpreted as being associated with such glass transitions. However, a few words of caution are appropriate. Brillouin scattering, by its very nature, entails detailed optical examination of the specimens. Hence, phenomena which are obvious in these circumstances might easily be missed by other techniques. For example, the phase separation, which we have observed near $T_g$ both visually as the milky iridescence and through the behaviour of the Brillouin width, might conceivably produce enthalpic events which could influence DSC thermograms and interfere with or confuse a simple interpretation of baseline shifts as evidence for glass transitions. Furthermore, the cracking of the specimens in the glass state may also be of significance, not only for thermal, but also other techniques of determining $T_g$, such as mechanical methods. The results obtained here suggest, therefore, that experimental measurements by such techniques on potential glassy systems should be interpreted with due caution.

Given that the sample is reasonably transparent to light, Brillouin spectroscopy is a powerful technique that can be applied to many aspects of glass transitions in food systems. In particular, the present study has shown that it can provide a measure of the glass transition temperature. It may be more elaborate and specialized than conventional methods of determining $T_g$, but if available, can be used to measure not merely $T_g$, but also the temperature dependence of the Brillouin shift $\nu_B$ and width $\Gamma_B$ in the system under study. These in turn depend on a large number of physical parameters including the refractive index, sound velocity, sound attenuation, elastic moduli and specific volume (5). These often provide corroborative evidence about the scattering system and simultaneous determination of these parameters frequently reveals much detailed information about the microscopic dynamics of systems undergoing glass transitions. The results reported here are consequently only one aspect of a more comprehensive study of Brillouin scattering in basic food materials, the full results of which will be reported later.

## References

1. Franks,F. (1985) In Simatos,D. and Multon,J.L. (eds) *Properties of Water in Foods*. Martinus Nijhoff, Dordrecht, p. 497.

2. Levine,H. and Slade,L. (1988) In Blanshard,J.M.V. and Mitchell,J.R. (eds), *Food Structure: Its Creation and Evaluation*. Butterworths, London, p. 149.
3. Wolanczyk,J.P. (1989) *Cryo-Lett.*, **10**, 73–76.
4. Ng,S.C., Hosea,T.J.C., Teh,H.C. and Gan,L.M. (1985) *J. Phys. E: Sci. Instrum.*, **18**, 250–252.
5. Ng,S.C., Hosea,T.J.C. and Goh,S.H. (1987) *Polym. Bull.*, **18**, 155–158.
6. French,D. (1984) In Whistler,R.L., Berniller,H.N. and Paschall,E.F. (eds), *Starch Chemistry and Technology*. Academic Press, New York. p. 183.
7. Hosea,T.J.C. and Ng,S.C. (1988) *J. Phys. C: Solid State Phys.*, **21**, 5317–5328.
8. Mitchell,R.S. and Guillet,J.E. (1974) *J. Polym. Sci., Polym. Phys. Ed.*, **12**, 713.
9. Zeleznak,K.J. and Hoseney,R.C. (1987) *Cereal Chem.*, **64**, 121–124.
10. Leutheusser,E. (1984) *Phys. Rev. A*, **29**, 2765–2773.
11. Levine,I.N. (1983) *Physical Chemistry*, 2nd edn. McGraw-Hill, New York, p. 827.
12. Orford,P.D., Parker,R., Ring,S.G. and Smith,A.C. (1989) *Int. J. Biol. Macromol.*, **11**, 91–96.